

## SLICED BEAM PARAMETER MEASUREMENTS

D. Alesini, E. Chiadroni, M. Castellano, L. Cultrera, G. Di Pirro, M. Ferrario, D. Filippetto, G. Gatti, L. Ficcadenti, E. Pace, C. Vaccarezza, C. Vicario, INFN/LNF, Frascati, Italy  
 B. Marchetti, A. Cianchi, University of Rome Tor Vergata and INFN-Roma Tor Vergata, Italy  
 A. Mostacci, University La Sapienza, Roma, Italy  
 C. Ronsivalle, ENEA C.R. Frascati, Italy

### Abstract

One of the key diagnostics techniques for the full characterization of beam parameters for LINAC-based FELs is the use of RF deflectors. With these devices it is possible to completely characterize both the longitudinal and the transverse phase space. In the paper we illustrate the main design considerations for time resolved (sliced) beam parameter measurements using RF deflectors (RFDs). Measurement setups for longitudinal pulse shape as well as phase space and transverse beam slice emittance characterizations are described. The main sources of error are discussed and the design criteria of these devices are presented. In particular the SPARC RF deflector and the related diagnostic lines as well as recent measurement results are shown. Measurement results obtained at LCLS and FLASH are then shortly illustrated.

### INTRODUCTION

The characterization of the longitudinal and transverse phase space of the beam at the end of an injector is a crucial point in order to verify and tune all photo-injector parameters. With the use of an RFD it is possible to measure the bunch longitudinal profile and, adding a dispersive system, the longitudinal beam phase space [1,2]. Similarly, since the longitudinal beam distribution can be projected along a transverse coordinate, the transverse emittance of each longitudinal bunch slice can be measured using the quadrupole scan technique [3]. In the first section of the paper we shortly review the basics principles of the longitudinal and transverse beam phase space characterization using an RFD. The main properties of both SW and TW deflecting structures in term of electromagnetic field configuration and performances are discussed in the second section. In the third section we illustrate the typical measurement setups and, in particular, those installed in the SPARC photo-injector [4]. The main measurement results obtained at SPARC are discussed in the fourth section. The last section shows some relevant results obtained at LCLS [5] and FLASH [6] and new proposed techniques.

### BEAM DIAGNOSTICS USING RFD

The different types of measurements that can be done with RFDs are based on the property of the transverse voltage ( $V_{DEFL}$ ) to introduce a correlation between the longitudinal coordinate of the bunch ( $t_B$ ) and the transverse one (vertical, in general) at the screen

position ( $y_S$ ). The phase of the deflecting voltage is chosen in order to have a zero crossing of the transverse voltage in the center of the bunch, giving a linear transverse deflection from the head and the tail of the bunch itself. After the deflector the transverse kick results into a transverse displacement of each longitudinal bunch slice, proportional to its position with respect to the bunch center. The mechanism is illustrated in Fig. 1.

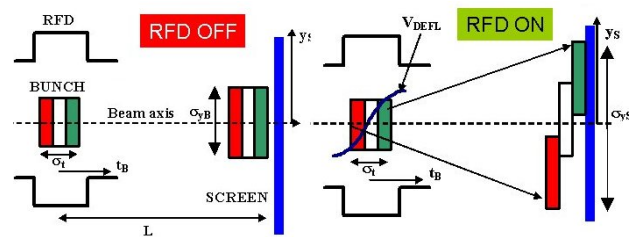


Figure 1: Longitudinal to transverse correlation induced by the RFD transverse voltage.

Since the beam has a finite transverse emittance, the distribution of the deflected bunch at the screen position is the superposition between the deflected beam profile and the transverse size of each bunch slice. In the plot we assumed that all longitudinal slices have the same transverse dimension on the screen ( $\sigma_{yB}$ ) and that there is a simple drift ( $L$ ) between the RFD and the screen. The total vertical rms distribution ( $\sigma_{yS}$ ) at the screen is simply given by [2]:

$$\sigma_{yS}^2 \cong K_{cal}^2 \sigma_{tB}^2 + \sigma_{yB}^2 \quad (1)$$

where  $K_{cal} = (V_{DEFL}/E)\omega_{RF}L$ ,  $\omega_{RF}$  is the angular frequency of the deflecting voltage and  $E$  is the beam energy in eV units. From this formula one can define the resolution length ( $\sigma_{tB-RES}$ ) as the bunch length that gives, on the screen, a distribution with rms vertical size equal to  $\sqrt{2}\sigma_{yB}$ . It is simply equal to:

$$\sigma_{tB-RES} = E \frac{\sigma_{yB}}{V_{DEFL} \omega_{RF} L} = \sqrt{E/E_0} \sqrt{\epsilon \beta_S} \frac{1}{V_{DEFL} \omega_{RF} L} \quad (2)$$

where  $\epsilon$  is the transverse normalized emittance of the beam,  $\beta_S$  is the vertical  $\beta$ -function at the screen position and  $E_0$  is the electron rest energy.

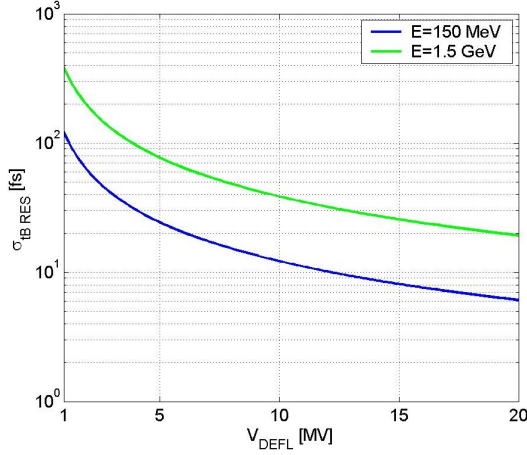


Figure 2: resolution as a function of the transverse deflecting voltage  $V_{\text{DEFL}}$ . Parameters:  $\epsilon=1$  [mm mrad],  $f_{\text{RF}}=2.856$  [GHz],  $\beta_S=1$  m,  $\sigma_{yB}\approx 18$   $\mu\text{m}$  (@1.5 GeV),  $\sigma_{yB}\approx 58$   $\mu\text{m}$  (@150 MeV),  $L=4$  m.

The plot of the resolution as a function of the transverse voltage is reported in Fig. 2 for the set of parameters reported in the figure caption and for two different energies. In the SPARC case, as example, we have that  $V_{\text{DEFL}}\approx 1.5$  MV,  $f_{\text{RF}}=2.856$  [GHz],  $\sigma_{yB}\approx 100$   $\mu\text{m}$ ,  $E\approx 150$  MeV and  $L\approx 4$  m, the typical resolution is then  $\sim 130$  fs. From Fig. 2 it is possible to observe that resolution of the order of few ten of fs are reachable with standard deflecting structures in the case of a 1.5 GeV beam and below ten fs in the case of a 150 MeV beam.

The other important characteristics of such system is that it is possible to self calibrate the measurements. The coefficient  $K_{\text{cal}}$  that relates the vertical coordinate at the screen with the time coordinate of the bunch can be, in fact, directly calculated measuring the bunch centroid position  $\langle y_S \rangle_{\text{meas}}$  on the screen for different values of the RFD phase by the formulae:

$$K_{\text{cal}} = \omega_{\text{RF}} \frac{\langle y_S \rangle_{\text{meas}_1} - \langle y_S \rangle_{\text{meas}_2}}{\Delta\phi_{\text{meas}_1} - \Delta\phi_{\text{meas}_2}} \quad (3)$$

Typical measurements of the calibration coefficient in the SPARC photo-injector are reported in Fig. 3 for different energies.

A careful discussion of other source of errors in the measurements with RFD is reported in [1,2].

## RF DEFLECTING STRUCTURES

Different types of deflecting structures can be used for beam diagnostics. As in the case of accelerating sections, the main differentiation is between the travelling wave (TW) and standing wave (SW) cavities. In general RFDs are multi-cell devices working on the  $\text{TM}_{11}$ -like mode [7,8]. In all type of structures both the electric ( $E$ ) and the magnetic ( $B$ ) field contribute to the total deflection. Figure 4 shows the two field components on axis ( $z$  is the propagation direction). In the plot we also reported the longitudinal electric field on the deflecting plane. From

the plot it is possible to observe that the deflecting modes have non-zero derivative of the longitudinal electric field on axis. We will discuss later the effect of such component in the measurements.

Since there are two possible polarities of the deflecting field, polarizing rod or holes are, in general, foreseen to introduce an azimuthal asymmetry in the structure fixing the working polarity itself [7,8].

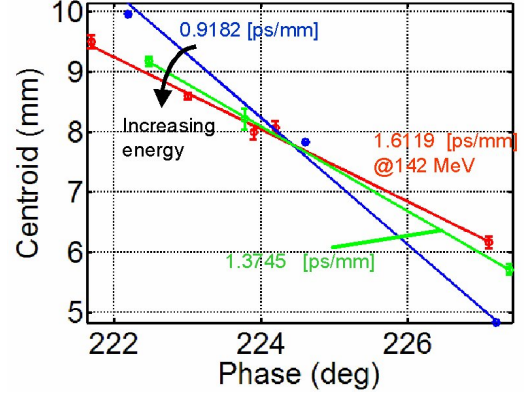


Figure 3: Typical measurements of the calibration coefficient in the SPARC photo-injector for different energies.

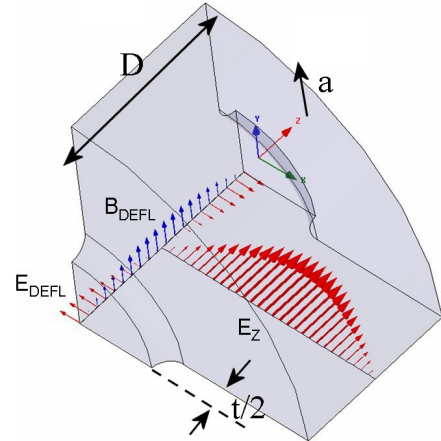


Figure 4: Single cell deflecting structure  $E$  and  $B$  field vectors.

Another important characteristic of the deflecting modes is that the transverse force is uniform over a wide region inside the iris aperture and is practically constant over a region with radius of  $a/2$ .

In TW devices the iris aperture ( $a$ ) is the most important parameter to fix the deflection efficiency, group velocity and the attenuation per unit length. Analytical expressions valid in the case of small pitch approximation ( $t \ll D$ ) [7,8] and can be very useful for a first evaluation of the deflecting structures parameters. Typical working mode is the  $2\pi/3$ . A detailed analysis of such structures is, for example, reported in [2].

SW structures are multi cell devices working, for example, on the  $\pi$ -mode. These structures have, in general a higher efficiency per unit length with respect to the TW ones but the maximum number of cells is limited

to few tens because of mode overlapping. Due to the resonant nature of their electromagnetic field, they require, in general, circulators to protect the RF source from reflections and they have higher filling times compared to the TW case.

Figure 5 shows, for example, the deflecting voltage and the maximum surface electric field for four types of structures working in S Band at 2.856 GHz. From the plot it is possible to observe that, because of the higher surface electric field, SW multi-cell devices can be used with input power below 10 MW giving  $V_{\text{DEFL}} < 7$  MV.

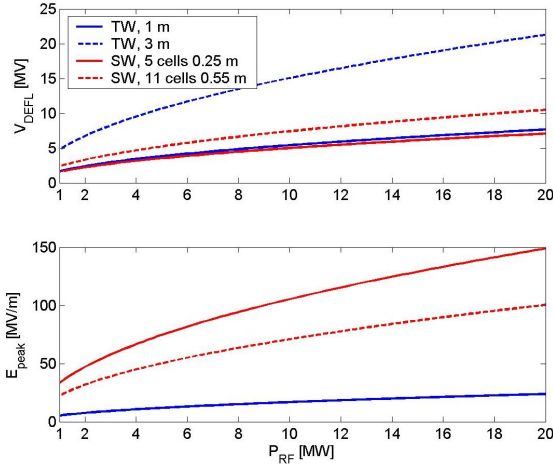


Figure 5: the deflecting voltage and the maximum surface electric field for four types of structures working in S Band at 2.856 GHz.

An example of SW structure is the SPARC RFD [9]. It is a 5 cells SW structure working on the  $\pi$ -mode at 2.856 GHz and fed by a central coupler with coupling coefficient equal to 1. Its transverse shunt impedance is  $\approx 2.5 \text{ M}\Omega$  and gives a deflection of 3 MV with an input power of 2 MW. It is now installed in the SPARC injector (as shown in Fig. 6) for beam diagnostics. More detail can be found in [9].

### Induced Energy Spread by RFD

The  $\text{TM}_{11}$ -like deflecting modes has a non-zero derivative of the longitudinal electric field on axis. This is a general property of the deflecting modes because the deflecting voltage is directly related to the longitudinal electric field gradient through the Panofsky-Wenzel theorem by the formula:

$$\tilde{V}_y = j \frac{c}{\omega} \int \nabla_y \tilde{E}_z e^{j \frac{\omega}{c} z} dz \quad (4)$$

Since this gradient is 90 deg out-of phase with respect to the deflecting voltage, it introduces an energy spread inside the bunch when the deflectors are used for beam diagnostics (in this case, in fact, the phase of the deflecting voltage is set to have zero crossing of the transverse voltage in the center of the bunch).

The contribution of the RFD to the slice energy spread is not negligible and, to the first order depends linearly on

the vertical slice size inside the RFD ( $\sigma_{yB\_RFD}$ ) and can be evaluated by the formula:

$$\sigma_{E\_RFD} \cong \frac{\omega_{RF}}{c} \hat{V}_{\text{DEFL}} \sigma_{yB\_RFD} \quad (5)$$

Typical values, in the case of SPARC, are of the order of 10-20 keV since  $\sigma_{yB\_RFD} \approx 300 \mu\text{m}$ .

The contribution of the deflector to the slice energy spread can be taken into account performing two measurements at two different deflecting voltages and using the following formulae to evaluate the sigma  $\sigma_{yB\_RFD}$  of each slice.

$$\sigma_{y\_RFD}^2 = \left( \frac{c}{\omega_{RF}} \right)^2 \frac{\sigma_{E\_MIS\_1}^2 - \sigma_{E\_MIS\_2}^2}{\hat{V}_{\text{DEFL}_1}^2 - \hat{V}_{\text{DEFL}_2}^2} \quad (6)$$

where  $\sigma_{E\_MIS\_1,2}$  are the two measured slice energy spreads.

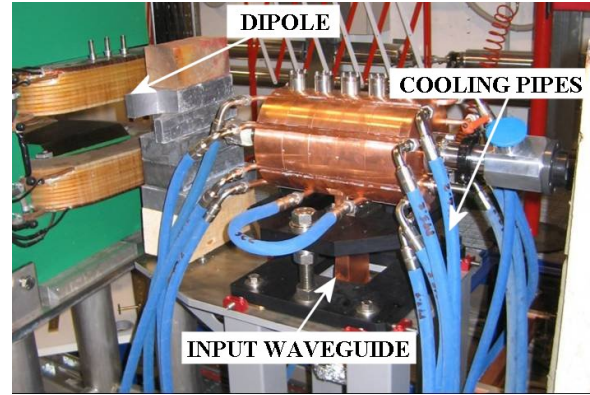


Figure 6: SPARC RFD installed in the LINAC.

## MEASUREMENT SETUP

### Slice Emittance and Beam Profile

The slice emittance is one of the fundamental parameter that defines the FEL process. It also contains important beam dynamics signature, revealing for instance if the emittance compensation process was performed at its best or not. The technique is similar to the usual quadrupole scan [3]. Because the RFD deflects the beam vertically a set of values for the quadrupoles must be found in advance to change only the horizontal dimension of the beam, keeping constant the vertical size in order to have the same longitudinal resolution.

The typical measurement setup is reported in Fig. 7. The picture and dimensions are referred to the SPARC diagnostics at the end of the 150 MeV LINAC. In case of beam profile and transverse slice emittance measurements the beam image is taken on the screen 1 and the slice beam emittance is measured by the quadrupole scan done by the triplet before the RFD. To correctly choose the quadrupole currents one has to previously measure the projected emittance and the twiss functions before the triplet (through an usual quad scan technique) and find the correct set of quadrupoles knowing the model of the beam line from the triplet to the screen 1.

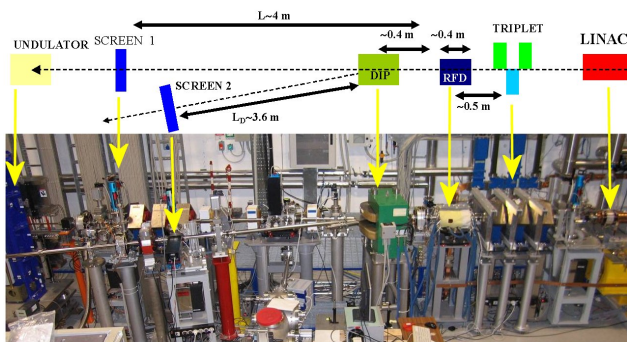


Figure 7: Typical measurement setup. The picture and dimensions are referred to the SPARC diagnostics.

### Longitudinal Phase Space

The longitudinal phase space can be characterized using the combination of RFD and dipole as illustrated in Fig. 7. In this case the beam is projected into the screen 2 and, also in this case, in order to have enough longitudinal resolution the vertical dimension at the screen position has to be taken under control. From the phase space picture the slice energy spread can be extrapolated by slicing the beam vertically and measuring the beam thickness in energy as function of time. Also the horizontal  $\beta$ -function at the screen 2 has to be reduced as much as possible in order to reduce the emittance contribution to the energy spread measurement. In any case the dominant systematic error is the energy spread induced by the RFD.

### MEASUREMENT RESULTS AT SPARC

The SPARC project is an R&D photo-injector facility for the production of high brightness electron beams to drive SASE and SEEDDED FEL experiments in the visible and UV light [10]. The high beam quality produced by SPARC will also allow investigations into the physics of ultra-short beams, plasma wave-based acceleration, and production of advanced X-ray beams via Compton back-scattering. The study of the beam slice properties, such as slice emittance or slice energy spread, allow to deeply investigate the details of emittance compensation method and to tune the machine for best performance. Moreover the knowledge of the beam current, beam energy, slice emittance and slice energy spread gives a complete description of the FEL process.

### Beam Profile

Several beam profile measurements have been done at SPARC in different operating condition. Here we report the results obtained during the velocity bunching experiment. The detail of the experiment is illustrated in [10]. The beam is injected in a long accelerating structure at the crossing field phase and it is slightly slower than the phase velocity of the RF wave. In this condition it slips back to phases where the field is accelerating, but at the same time it is chirped and compressed.

The longitudinal beam profile measurements are crucial for this experiment because, while the bunch is

compressed, it also change its longitudinal distribution. Figure 8 shows the measured compression ratios versus injection phase in the first travelling wave structure. The red curve has been obtained with PARMELA simulation. The error bars in figure have been computed over the 10 images collected for each measurement, a more detailed study including jitters effects and systematic error will be the subject of future investigations.

We have been operating with a quasi-Gaussian longitudinal laser profile  $\sim 7.5$  ps FWHM long with 300  $\mu\text{m}$  transverse spot size. The bunch charge was 300 pC. The beam acceleration on crest corresponds to the phases around  $-75$  deg. In this condition the measured longitudinal profiles compared with the PARMELA simulation are reported in Fig. 9 (a), the rms bunch length is length measured at the linac exit was  $\sim 3.25$  ps with energy of 150 MeV. The beam profile compared with simulation in the case of a compression factor equal to 3 (inj. Phase= $-87$  deg) is reported in Fig. 9 (b).

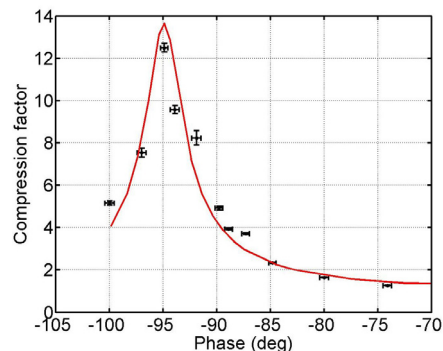


Figure 8: Compression factor versus injection phase, experimental points and PARMELA simulations (red curve).

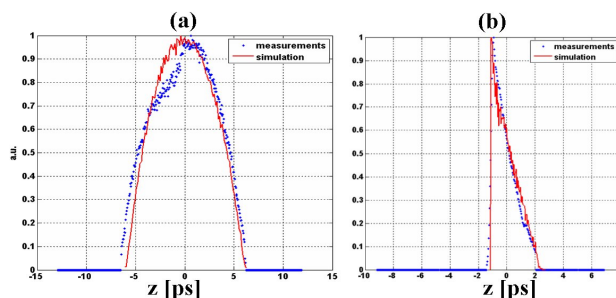


Figure 9: Beam profiles in the velocity bunching experiment @ SPARC; (a) not compressed beam, (b)compression ratio 3.

### Slice Emittance

In the plot of Fig. 10 we compare the slice emittance measurement with a beam with 125 pC of charge and a laser spot on the cathode of 320X300  $\mu\text{m}$  with a PARMELA simulation. In this plot we used a technique that we called RUS (Running Slice). It is very hard, especially on the beam tails, to determine the first and the last slice. This assumption however has impact on the position of all the other slices. To overcome this problem and resolve the ambiguity we fix a slice length (in our

case 200  $\mu\text{m}$ ) and move it along the bunch in step of about 500 fs.

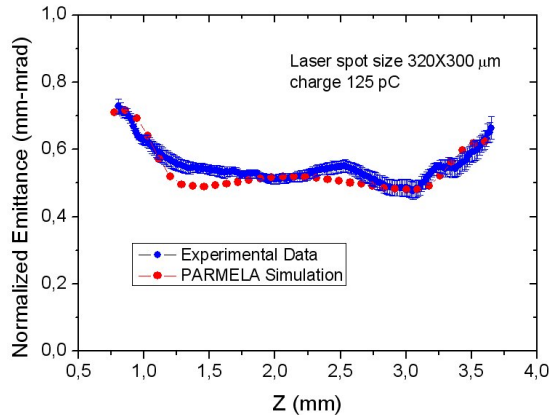


Figure 10: Comparison between slice emittance measurements and PARMELA simulation.

### Longitudinal Phase Space

A typical longitudinal phase space measurements is reported in Fig. 11. From the plot the slice energy spread has been extrapolated and is given in Fig. 12, compared with simulations. The main discrepancy between the simulations and the experimental data is given by the RFD contribution that has been estimated by the formula (5) to be  $\sim 15$  keV. The emittance contribution has not been subtracted from the measurements, but it has been estimated to be less than 10%.

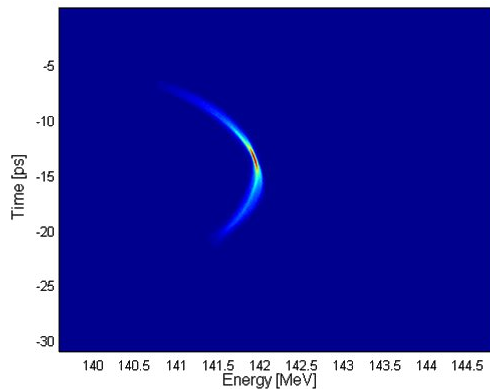


Fig. 11: Longitudinal trace space at 140 MeV.

## EXPERIMENTAL RESULTS IN OTHER ACCELERATOR FACILITIES

New important results have been also reached in other accelerator facilities like LCLS or FLASH. In the first case two TW deflecting structures (LOLA type) are installed in the LINAC and allow measurements at low (135 MeV) and high energies (13.5 GeV). By RFD structures several important measurement have been done like the measurement of the increment in the energy spread by laser heating, slice emittance, or verification of the effect of the X-Band cavity in the correction of the chirp in the energy distribution of the beam [5]. Several measurements have been also done at FLASH by a TW 3.6 m long cavity at the end of the injector [6]. Beam

profiles and slice emittances in different operating conditions have been done with resolution of the order of 20 fs. Very promising results have been also reached few years ago with circular polarized RF deflectors. [11]. In this case with the same device it is possible to simultaneously measure the longitudinal phase space (without introducing energy spread errors) and the beam profiles. Recent interesting new techniques in the deflecting cavities fabrication adopting aluminium have been also explored [12].

## CONCLUSIONS

RFDs are crucial devices for both longitudinal and transverse phase space characterization allowing reaching resolution below 10 fs. The measurement setups and the experimental results, in the case of SPARC, have been shown and discussed. In particular the use of the RFD technique has been fundamental in the velocity bunching experiment at SPARC. A possible solution to take into account the contribution of the RFD in the energy spread slice has been also illustrated. Important new results have been also reached in other accelerator facilities like LCLS or FLASH and the use of the RFD technique allowed measuring laser heating effects or longitudinal phase space correction using X-Band cavities.

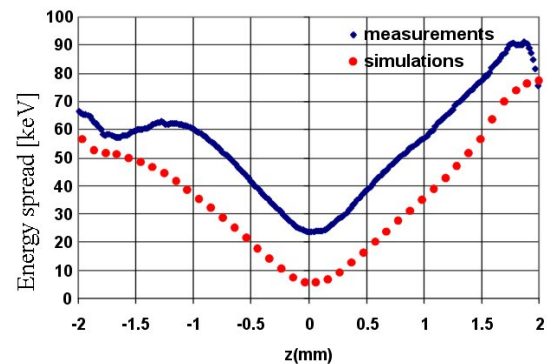


Figure 12: Measurements of the slice energy spread.

## ACKNOWLEDGEMENTS

The authors would like to acknowledge P. Emma, C. Gerth and M. Rohrs for the information's and material on LCLS and FLASH measurement results.

## REFERENCES

- [1] P. Emma, et al., LCLS-TN-00-12, 2000.
- [2] D. Alesini, IJMPA, Vol. 22 No: 22 Year: 2007.
- [3] M. Minty and F. Zimmermann, Springer, 2003.
- [4] B. Marchetti, et al., to be published in Proc. of PAC 09.
- [5] P. Emma, et al., to be published in Proc. of PAC 09.
- [6] M. Rohrs, et al., Proc. of EPAC 06 and FEL 05.
- [7] P. Bernard and H. Lengeler, CERN 68-30, 1968.
- [8] G. A. Loew, et al., SLAC Report 17, 1963
- [9] D. Alesini, et al., NIM A, 2006.
- [10] M. Ferrario et al., to be published in Proc of PAC 09.
- [11] J. Haimson, et al., AIP Conf. Proc. 647, 2002.
- [12] D. Alesini, to be published in Proc. of PAC 09.